J. Anat. (2010) **216**, pp121–131 doi: 10.1111/j.1469-7580.2009.01175.x

Variation in within-bone stiffness measured by nanoindentation in mice bred for high levels of voluntary wheel running

Kevin M. Middleton,[1,3,*] Beth D. Goldstein,[2,‡] Pradeep R. Guduru,[2] Julie F. Waters,[2] Scott A. Kelly,[3,‡] Sharon M. Swartz[1,2] and T. Garland Jr[3]

[1]*Department of Ecology and Evolutionary Biology, Brown University, Providence, RI, USA*
[2]*Division of Engineering, Brown University, Providence, RI, USA*
[3]*Department of Biology, University of California, Riverside, Riverside, CA, USA*

Abstract

The hierarchical structure of bone, involving micro-scale organization and interaction of material components, is a critical determinant of macro-scale mechanics. Changes in whole-bone morphology in response to the actions of individual genes, physiological loading during life, or evolutionary processes, may be accompanied by alterations in underlying mineralization or architecture. Here, we used nanoindentation to precisely measure compressive stiffness in the femoral mid-diaphysis of mice that had experienced 37 generations of selective breeding for high levels of voluntary wheel running (HR). Mice (n = 48 total), half from HR lines and half from non-selected control (C) lines, were divided into two experimental groups, one with 13–14 weeks of access to a running wheel and one housed without wheels (n = 12 in each group). At the end of the experiment, gross and micro-computed tomography (μCT)-based morphometric traits were measured, and reduced elastic modulus (E_r) was estimated separately for four anatomical quadrants of the femoral cortex: anterior, posterior, lateral, and medial. Two-way, mixed-model analysis of covariance (ANCOVA) showed that body mass was a highly significant predictor of all morphometric traits and that structural change is more apparent at the μCT level than in conventional morphometrics of whole bones. Both linetype (HR vs. C) and presence of the mini-muscle phenotype (caused by a Mendelian recessive allele and characterized by a ~50% reduction in mass of the gastrocnemius muscle complex) were significant predictors of femoral cortical cross-sectional anatomy. Measurement of reduced modulus obtained by nanoindentation was repeatable within a single quadrant and sensitive enough to detect inter-individual differences. Although we found no significant effects of linetype (HR vs. C) or physical activity (wheel vs. no wheel) on mean stiffness, anterior and posterior quadrants were significantly stiffer ($P < 0.0001$) than medial and lateral quadrants (32.67 and 33.09 GPa vs. 29.78 and 30.46 GPa, respectively). Our findings of no significant difference in compressive stiffness in the anterior and posterior quadrants agree with previous results for mice, but differ from those for large mammals. Integrating these results with others from ongoing research on these mice, we hypothesize that the skeletons of female HR mice may be less sensitive to the effects of chronic exercise, due to decreased circulating leptin levels and potentially altered endocannabinoid signaling.

Key words artificial selection; bone; exercise; experimental evolution; material properties; nanoindentation.

Introduction

Bone as a composite

The overall behavior of bone under mechanical loading is a function of structure and material constituents on both macro and micro scales. Moreover, the composite nature of bone (Lakes, 1993; Currey, 2003; Ji & Gao, 2004; Tai et al. 2007), coupled with the potential for alterations of its structure and material properties under the influence of specific sets of alleles (Kodama et al. 2000; Robling et al. 2003, 2007; Akhter et al. 2004; Lang et al. 2005; Ralston et al.

Correspondence
Kevin M. Middleton, Department of Biology, California State University, San Bernardino, 5500 University Parkway, San Bernardino, CA 92407, USA. T: + 1 909 5375577; F: + 1 909 5375305; E: kmm@csusb.edu
Present addresses:
*Department of Biology, California State University, San Bernardino, San Bernardino, CA, USA;
‡Jefferson Medical College, Thomas Jefferson University, Philadelphia, PA, USA;
‡Department of Nutrition, University of North Carolina, Chapel Hill, Chapel Hill, NC, USA.

Accepted for publication *16 October 2009*

2005; Bower et al. 2006; Kesavan et al. 2006, 2007; Beamer et al. 2007; Jiao et al. 2007) and exercise (Kodama et al. 2000; Kesavan et al. 2005, 2006, 2007; Kelly et al. 2006; Robling et al. 2007), suggests that bone has the potential to respond across multiple generations (i.e. evolutionary change) or within an individual's lifetime (i.e. phenotypic plasticity) on multiple spatial scales, from micro-scale material constituents to macro-scale morphology.

Mouse model of voluntary exercise

Studies of bone biomechanics in mice traditionally have compared inbred strains of mice (Robling & Turner, 2002; Koller et al. 2003; Robling et al. 2003), mice with specific gene knockouts (Hamrick et al. 2000, 2006) or transgenic animals (Akhter et al. 2004; MacDonald et al. 2007). Here, we employ a novel experimental mouse model to study skeletal biomechanics on two spatial scales. We use a large-scale and long-term (> 15 year) artificial selection experiment for high voluntary wheel running in which changes in bone macrostructure, material properties and, ultimately, response to loading could be a result of changes in genetic architecture (i.e. a correlated response to selection), variation in the environment (i.e. effects of training) or a combination (Swallow et al. 1998, 2009; Garland, 2003; Middleton et al. 2008a). In addition, the magnitude of the response to exercise training may itself be genetically controlled (Garland & Kelly, 2006; Middleton et al. 2008a).

Our previous work using this model system has demonstrated significant morphological changes in skeletal traits resulting from both selective breeding and access to a running wheel, and from the interaction of these factors. Mice from the four replicate High Runner (HR) lines (those bred for high voluntary wheel running) exhibit significantly wider distal femoral condyles (Kelly et al. 2006; Middleton et al. 2008b), significantly larger femoral heads (Kelly et al. 2006; Middleton et al. 2008b), and significantly less directional asymmetry of hind limb bone lengths (Garland & Freeman, 2005) when compared with four non-selected control (C) lines. By housing HR and C mice with and without access to running wheels, the effects of genetics and physical exercise can be studied simultaneously. In response to 8 weeks of wheel access, Kelly et al. (2006) found significant increases in anteroposterior and mediolaterial minimum tibial and femoral diameters, as well as anteroposterior diameter of the femoral head (see also further analyses in Middleton et al. 2008a).

Phenotypic adaptation in response to loading

Because the response of bone to *in vivo* loading is a function not only of the geometric distribution of bony material but also the mechanical properties of that material, gross morphological changes in a the structure of a bone may be accompanied by alterations in the underlying material of which the bone is composed. Commonly, three- and four-point bending have been used to assess bone mechanical properties (e.g. Broz et al. 1993; Robling & Turner, 2002; Babij et al. 2003; Koller et al. 2003; Akhter et al. 2004). However, these methods often suffer from the assumption of isotropy (Silva et al. 2004). Recently, nanoindentation has emerged as a powerful technique for assessing the micromechanical properties of bone. Early studies (Rho et al. 1997, 1999a,b; Roy et al. 1999; Turner et al. 1999; Zysset et al. 1999) were designed to refine the methodology and probe the mechanical properties of cortical and trabecular bone, but more recent studies have used nanoindentation to compare bone material properties on a finer scale, for example, in different strains of mice (Akhter et al. 2004; Silva et al. 2004). In senescence-accelerated mice, Young's moduli estimated from four-point bending were found to be five times lower than those computed from nanoindentation, perhaps because of the porosity of whole bone (Rho et al. 2002; Silva et al. 2004). More widespread acceptance of nanoindentation as one method for assessing comparative micro-scale mechanical properties of bone is evidenced by recent studies with direct relevance to human biological systems (Fan et al. 2007; Kavukcuoglu et al. 2007; Tai et al. 2007; Amanat et al. 2008; Leong & Morgan, 2008; Nazarian et al. 2008).

Here, we combine studies of gross and micro-computed tomography (μCT)-derived morphometric traits with direct estimates of bone stiffness from nanoindentation to compare the morphology and mechanical behavior of femoral cortical bone in HR and C mice reared in two different environments, with or without access to a running wheel. We hypothesized that gross morphological changes would be accompanied by underlying alterations of tissue architecture, which would be reflected by significantly different elastic moduli. We also present a systematic methodology for detecting outliers among a large sample of indents and assess the repeatability of stiffness estimation by nanoindentation in a single sub-region of a bone. Finally, methods for detecting intra-specimen and intra-bone differences in stiffness are discussed.

Materials and methods

Model system

Mice used in this study were part of a long-term artificial selection experiment on voluntary wheel-running behavior (Garland, 2003; Rhodes et al. 2005; Swallow et al. 2009). The complete experimental design and rationale is described elsewhere (Swallow et al. 1998; Garland, 2003), and here we provide only an overview.

The experiment consists of eight closed lines established from an outbred base population of ICR strain mice (Harlan Sprague Dawley, Indianapolis, IN). Genetic variation in the founder population was essential to allow gene frequencies to change across generations (Eisen, 1987, 1992; Eisen et al. 1995; Bennett, 2003), precluding the use of an inbred mouse strain. Four of the eight

lines were designated as non-selected controls (C), and the other four were designated as high runner (HR) lines in which the parents of subsequent generations are those mice that exhibit the highest levels of voluntary wheel running during the 5th and 6th days of a 6-day exposure to wheels. Summed revolutions on days 5 and 6 increased rapidly in HR lines relative to control lines, such that, after 16 generations, HR lines ran 170–200% more revolutions than control lines (Garland, 2003; Swallow et al. 2009). In addition to changes in wheel-running behavior, numerous correlated responses have been observed in behavior (Carter et al. 2000; Gammie et al. 2003; Malisch et al. 2009), physiology (Dumke et al. 2001; Rezende et al. 2006a,b), and endocrinology (Girard & Garland, 2002; Girard et al. 2007; Malisch et al. 2007, 2008), many of which (e.g. home-cage activity levels, glucose uptake rate, leptin levels) may have relevance to skeletal physiology (also see Discussion below). Selection is unidirectional (only for high levels of voluntary wheel running), and comparisons are made only between HR mice and their non-selected controls. Several potential difficulties argue against implementing selection for reduced wheel running, including unintentional selection on non-performance traits (e.g. fearfulness of running wheels) or for increases in alleles deleterious to overall health (see Garland, 2003 for additional discussion).

A subset of HR mice exhibit a 'mini-muscle' (MM) phenotype, which is characterized by an approximate 50% reduction in the mass of the triceps surae muscle complex (Garland et al. 2002; Houle-Leroy et al. 2003). A simple Mendelian recessive allele (Garland et al. 2002; Hannon et al. 2008), the mini-muscle (MM) allele, has been mapped to a 2.6-Mb region of mouse chromosome 11 (MMU11; Hartmann et al. 2008). In addition to changes in muscle mass and contractile physiology (Houle-Leroy et al. 2003; Syme et al. 2005; Guderley et al. 2006, 2008), mice exhibiting the MM phenotype have significantly longer and thinner femora and tibiae (Kelly et al. 2006). However, the dry mass of these bones is not lower than that of control mice.

Study population

Female mice (n = 24 from HR lines) from generation 37 of selection and controls (n = 24 from control lines) were given access to a running wheel (n = 12 HR; n = 12 control) or not (n = 12 HR; n = 12 control), beginning at a mean age of 79 days (range = 74–81 days). Food and water were available *ad libitum*. For wheel-access mice, the number of wheel revolutions was recorded by computer in 1-min bins using an automated system (Swallow et al. 1998). After 13–14 weeks, mice were sacrificed and stored at −20 °C until dissection. Mean age at sacrifice was 174 days (range = 171–177 days). All procedures were reviewed and approved by the IACUC of the University of California, Riverside, an AAALAC-accredited institution.

Morphometric measurements and μCT scanning

After thawing, right and left femora were dissected free of the surrounding tissue and manually defleshed. Morphometric traits of the femur measured were: proximal width from the femoral head to the lateral aspect, distal width at the femoral condyles, mediolateral and anteroposterior diameters at the femoral mid-diaphysis, proximodistal and anteroposterior diameters of the femoral head and neck (also see Fig. 1 in Middleton et al. 2008b). All measurements were made using digital calipers (Mitutoyo Corporation) to the nearest 0.01 mm. Femora were then frozen separately in 0.9% saline at −20 °C.

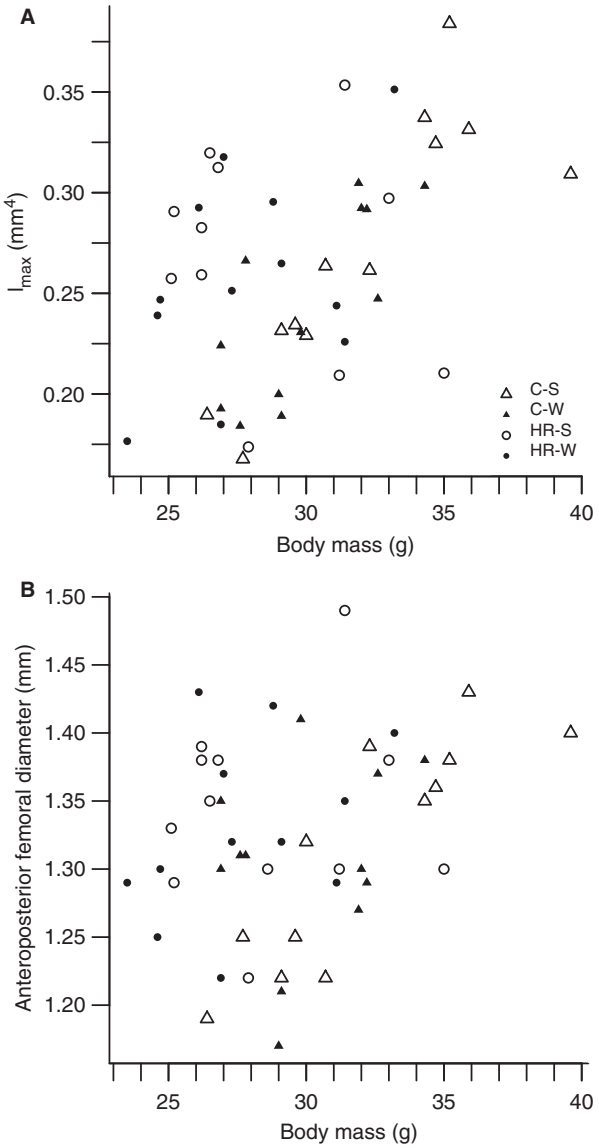

Fig. 1 Plots of (A) I_{max} vs. Body mass and (B) Anteroposterior (AP) femoral diameter vs. Body mass coded by control (C)/High Runner (HR) and wheel-access (W) or no wheel-access (S, sedentary). Results of two-way ANCOVA (Table 1) reveal significant differences between control and HR mice in I_{max} (A; P = 0.0207) but not in AP diameter (B; P = 0.3809; see Table 1).

Cross-sectional anatomy of the femoral mid-diaphysis was imaged using a high-resolution fan-beam μCT scanner (μCT 40; Scanco Medical AG, Bassersdorf, Switzerland). Cross-sectional areas, maximum and minimum second moments of area (I_{max} and I_{min}, respectively), maximum section moduli (I_{max}/C_{min}, where C_{min} is the maximum extent of the material perpendicular to I_{min}), and minimum section moduli (I_{min}/C_{max}, where C_{max} is the maximum extent of the material perpendicular to I_{max}) were calculated using the built-in software of the μCT scanner from eight consecutive slices of the femoral mid-diaphysis (voxel size = 9 μm^3).

Nanoindentation

Sample preparation

Femora were embedded in low viscosity epoxy (EPO-THIN; Buehler Ltd., Lake Bluff, IL) at room temperature. A ~0.5-mm section was cut from the femoral mid-diaphysis using a diamond saw (IsoMet Plus Precision Saw; Buehler Ltd.). Sections were mounted on microscope slides with paraffin, and polished by hand (Metaserv 2000 Grinder Polisher; Buehler Ltd.) using silicon carbide paper of progressively finer grit (400, 600, 800, 1200). Following hand polishing, cross-sections were removed from the paraffin mount and affixed to 15-mm stainless steel discs (Ted Pella, Inc., Redding, CA) with cyanoacrylate adhesive.

Discs were glued to the polishing mount of an automated polisher (Automet 2000, Buehler Ltd.) and polished on cloths using 5, 1 and 0.3 μm alumina suspensions (Texmet 1500 cloths, Masterprep Polishing Suspension; Buehler Ltd.). Final polishing was performed using a 0.5-μm alumina suspension and a separate cloth. Between polishing solutions, samples were rinsed thoroughly and dried with a stream of air. After polishing, samples were ultrasonically cleaned for 5 min in deionized water to remove surface debris. Adequate degree of polishing was verified using interferometry (NewView 5000; Zygo Corporation, Middlefield, CT).

Sample testing

Reduced elastic modulus (E_r) was measured using the method of Oliver & Pharr (1992) in each of four anatomical quadrants (anterior, posterior, medial, and lateral) by nanoindentation (TI 900 TriboIndenter; Hysitron Inc., Minneapolis, MN). E_r of a specimen is related to the elastic modulus of a specimen by the following equation:

$$\frac{1}{E_r} = \frac{(1-\nu^2)}{E} + \frac{(1-\nu_i^2)}{E_i}$$

where ν is Poisson's ratio for the indented specimen, ν_i is Poisson's ratio of the indenter material (here $\nu_i = 0.07$), and E_i is the elastic modulus of the indenter material (here $E_i = 1440$ GPa) (Oliver & Pharr, 1992). Experimentally, E_r is calculated from the slope of a line tangent to the load vs. displacement curve at peak indentation load. Specimens were examined visually under light microscopy to select suitable locations for indentation. Indents were made at the mid-point of the cortical bone, away from obvious osteocyte lacunae. Nine indents were made using a diamond Berkovich tip (~200 nm tip radius) in a 3×3 grid with 5-μm spacing between indents. Indents were made using a triangular load pattern to a maximum load of 1500 μN with a loading rate of 100 μm min^{-1}, which produced vertical displacements of 200–250 nm.

Because we were primarily interested in inter-individual and intra-bone variation rather than absolute magnitude of measured stiffness, we did not prevent samples from dehydrating during testing, although a 'hydrated nanoindentation' technique has been described previously (Rho & Pharr, 1999; Zysset et al. 1999; Hengsberger et al. 2002). All samples received similar treatment, hence we conclude that variation in reduced moduli arose from biological differences and not from specimen handling. Because our tests were made on dehydrated samples, we expect that the true elastic modulus of fully hydrated bone would be 10–24% lower than the values recorded here (Evans & Lebow, 1951; Ryan & Williams, 1989).

Statistical analysis

Morphometric and nanoindentation data were analyzed using two-way, mixed model ANOVAs and ANCOVAs in SAS PROCEDURE MIXED (Ver. 9.3; SAS Institute, Cary, NC) with Type III tests of fixed effects. Main effects tested for differences between HR and C mice (linetype effect), differences between wheel-access and no wheel-access mice (activity effect), their interaction (linetype × activity effects), and presence of the mini-muscle phenotype. For mice with wheel access, quantitative wheel running (mean revolutions per day) during the last 7 days prior to sacrifice was included as a covariate. Body mass was included as a covariate in all ANCOVA analyses because HR mice are smaller than C mice (Swallow et al. 1999) and because body mass is a strong predictor of overall size of skeletal elements (Kelly et al. 2006; Middleton et al. 2008a,b).

Because we performed many statistical tests on closely related data, our Type I error rate for the entire experiment may exceed the nominal 5% alpha level (Curran-Everett, 2000; Curran-Everett & Benos, 2004). To address this concern, we performed a positive false discovery rate (pFDR) analysis using the QVALUE package (Version 1.1; Storey, 2002) for R (Version 2.8.0; R Core Development Team, 2008), allowing for 5% false significant results (pFDR = 0.05). Based on the results of this analysis, a more appropriate and conservative alpha level for significance is $\alpha = 0.029$.

Results

Morphometrics

Body mass was a highly significant covariate in all analyses. After statistically accounting for body mass, significant differences in femoral cross-sectional geometry were observed (Table 1; Fig. 1A), both when comparing HR to C mice and when comparing those exhibiting the mini-muscle phenotype to those without. HR mice have significantly larger maximum second moments of area and minimum section moduli after controlling for body mass. After controlling for multiple comparisons, maximum section modulus is only suggestive of being increased in HR mice. In contrast, mice exhibiting the mini-muscle phenotype exhibit significantly smaller maximum second moments of area and maximum and minimum section moduli after controlling for body mass, selection, and activity status.

Nanoindentation

Identification of outliers

We calculated reduced modulus for 1694 total indents in the sample of 48 mice (only eight indents were available for some quadrants). Prior to statistical analysis, reduced modulus was $\log_{10}$ transformed to improve normality of residuals from the statistical models. A nested one-way ANOVA (quadrant nested within mouse) was used to objectively detect statistical outliers. Standardized residuals were calculated for the ANOVA model, and indents with standardized residuals greater than 3.5 or less than −3.5 were excluded from further analysis, which left 1672 measurements of reduced modulus.

Table 1 Results of two-way, mixed-model ANCOVA testing for main effects of Linetype (HR vs. C), Activity (wheel access vs. no wheel access), their interaction, and Mini-muscle phenotype (present vs. absent), with body mass (log_{10} transformed) as a covariate.

Trait	Linetype	Activity	Linetype × Activity	Mini-muscle	Body mass
ML femoral diameter	0.1109+	0.5494−	0.6561	0.1119−	**0.0001**
AP femoral diameter	0.3809+	0.3928+	0.6890	0.1470+	**<0.0001**
Width of the distal femoral condyles	0.1747+	0.5226+	0.8821	0.9814+	**<0.0001**
Proximal femoral width	0.1414+	0.2502−	0.1097	0.5002−	**0.0047**
Height of the femoral head	0.1192+	0.7981+	0.8828	0.3141−	**0.0006**
AP depth of the femoral head	0.1903+	0.9323−	0.2638	0.2521−	**<0.0001**
Cross sectional area	0.6006+	0.5661−	0.1953	0.1097−	**<0.0001**
I_{max}	**0.0207**+	0.5917−	0.7456	**0.0056**−	**<0.0001**
I_{min}	0.0928+	0.7087−	0.7880	0.3820−	**<0.0001**
Maximum section modulus	0.0361+	0.5338−	0.5492	**0.0149**−	**<0.0001**
Minimum section modulus	**0.0122**+	0.6025−	0.6474	**0.0019**−	**<0.0001**

Two-tailed *P*-values (not corrected for multiple comparisons) are shown, along with direction of the response (+ or −) for each comparison listed above. For example, I_{max} is significantly larger in HR mice than in C mice ($P = 0.0207$).

Repeatability and sequence effects

Repeatability of E_r estimated by nanoindentation was calculated for each anatomical region separately. Repeatability in this sense is calculated from a one-way ANOVA as (variance among mice)/(variance among mice + variance within mouse) (Lessels & Boag, 1987). If within-group variance is small, then this ratio is closer to 1, indicating a high repeatability. Repeatability values ranged from 0.66 for the lateral quadrant to 0.73 for the medial quadrant, indicating that the among-group variance (i.e. mouse-to-mouse differences) is 66–73% of the total variance.

A mixed-model ANOVA of all indents, using measurement sequence as a random effect nested within quadrants, revealed no significant effect of sequence (indent #1 to indent #9; $P = 0.2157$) but did show significant differences among mice ($P < 0.001$), among quadrants within mice ($P < 0.0001$), and in the interaction of mouse by quadrant ($P < 0.001$). Because we found both acceptably high repeatability and no sequence effect, we calculated a mean reduced modulus for each quadrant for each mouse and used that value for all remaining analyses.

Reduced modulus measured by nanoindentation

Among mice with wheel access, quantitative wheel running (mean revolutions per day) during the last 7 days prior to sacrifice was not a significant predictor of bone stiffness in either C ($P = 0.2095$) or HR lines ($P = 0.7633$), nor were replicate lines significantly different from one another (one-way ANCOVA; control: $P = 0.7300$; HR: $P = 1.0$).

When reduced modulus is predicted separately for each of the four quadrants (with mini-muscle phenotype as an additional main effect and body mass as covariate), no significant effects in either the anterior or medial quadrants were found (Table 2). In the lateral quadrant, E_r was significantly negatively correlated with body mass ($P = 0.029$), and in the posterior quadrant, presence of the MM phenotype was a nearly significant positive predictor of E_r ($P = 0.052$; Table 2).

An ANCOVA (body mass as covariate) in which mean E_r was modeled by quadrant, linetype, activity, their interaction and the mini-muscle phenotype, revealed a significant quadrant effect ($P = 0.0002$; Table 2, line 1), but no significant effects of linetype, activity, their interaction,

Table 2 Results of two-way, mixed model ANCOVA for the main effects of Linetype (HR vs. C), Activity (wheel access vs. no wheel access), their interaction, and Mini-muscle phenotype (present vs. absent) on mean reduced modulus (log_{10} transformed) for each bone quadrant analyzed separately, with body mass (log_{10} transformed) as a covariate.

Quadrant	Linetype	Activity	Linetype × Activity	Mini-muscle	Body mass	Quadrant
	0.9551+	0.5269−	0.3552	0.2112+	0.4448−	0.0002
Anterior	0.1829+	0.7728−	0.7100	0.4578−	0.4832+	
Posterior	0.2065−	0.5019−	0.4108	0.0524+	0.5092−	
Lateral	0.3595−	0.3372−	0.3239	0.2708+	0.0292−	
Medial	0.2790+	0.4077+	0.7791	0.9452+	0.1427+	

Two-tailed *P*-values (not corrected for multiple comparisons) are shown, along with direction of the response (+ or −) for each comparison listed above. The first row shows the results of a model fit with quadrant as an additional main effect (one level for each quadrant). In this model, quadrant was a significant overall predictor or bone stiffness (see text for details).

mini-muscle phenotype or body mass were found. *Post-hoc* analysis showed that the anterior and posterior quadrants, considered as a group, are significantly stiffer than the medial and lateral quadrants ($P < 0.0001$; Fig. 2). Moduli in the anterior and posterior quadrants do not differ significantly from one another ($P = 0.6431$), nor do those of the medial and lateral quadrants ($P = 0.4125$). Backtransformed least-squares means and 95% confidence intervals for the reduced moduli of each quadrant are shown in Table 3.

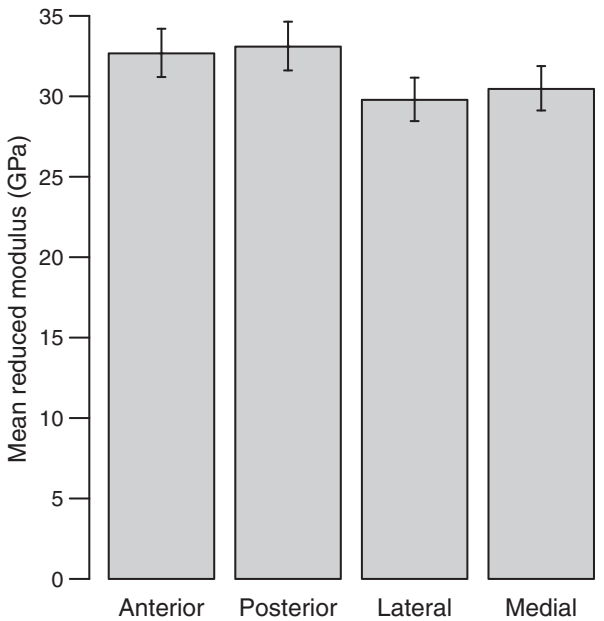

Fig. 2 Comparison of reduced modulus (E_r) and 95% confidence intervals for each of the four anatomical quadrants (backtransformed from $\log_{10}$ transformed raw data; also see Table 3). Anterior and posterior quadrants are significantly stiffer ($P < 0.0001$) than lateral and medial quadrants, but in neither pair is one mean significantly different from the other (anterior vs. posterior $P = 0.6431$; medial vs. lateral $P = 0.4125$).

Table 3 Least-squares means and 95% confidence intervals of reduced modulus (GPa; backtransformed from $\log_{10}$ transformed values) from two-way, mixed-model ANCOVA for the main effects of Linetype (HR vs. C), Activity (wheel access vs. no wheel access), Mini-muscle phenotype (present vs. absent), and Quadrant, with body mass as covariate (see Table 2, line 1).

Quadrant	Lower 95% CI	Least-squares mean	Upper 95% CI
Anterior	31.20	32.67	34.20
Posterior	31.61	33.09	34.64
Lateral	28.46	29.78	31.16
Medial	29.12	30.46	31.88

Discussion

Morphometrics

Our previous work using this model system, including studies of bones from animals sampled at different points during the many generations of selection and from animals with varying periods of wheel-access, has revealed significant morphometric differences between high runner and control lines of mice, mice housed with vs. without wheel access, and between normal and mini-muscle individuals (Garland & Freeman, 2005; Kelly et al. 2006; Middleton et al. 2008b). These gross morphological differences between (i) HR and C mice and (ii) active and non-wheel-active mice led us to hypothesize that such variation might also be reflected in material properties of the bone itself, despite the differences in generation of selection and length of wheel-access.

In this specific sample of mice – females from generation 37 of selection that were or were not given access to a running wheel for 13–14 weeks – we found differences in morphometric traits consistent with those found in other samples (Garland & Freeman, 2005; Kelly et al. 2006; Middleton et al. 2008b). μCT measurements of the cross-sectional properties of the femur are generally more sensitive than external bone dimensions, and, in this study, were able to detect more subtle differences among groups (Table 1; Fig. 1). Cross-sectional geometry may be more responsive to changes in bone loading than bone material properties, and thus more directly reflect the mechanical environment of the limb (Table 1; also see Carlson & Judex, 2007).

As we continue to accumulate diverse data on skeletal traits in mice from this ongoing selection experiment, we have discerned patterns we had not originally hypothesized. Whereas Kelly et al. (2006) analyzed only male mice (with/without 8–9 weeks of wheel access), this study and that described by Middleton et al. (2008b) included only females. Mice from the present study and that by Kelly et al. (2006) had wheel access for roughly comparable periods of time. In the sample of male mice analyzed by Kelly et al., wheel access affected many aspects of bone geometry: 14 of 22 traits studied differed significantly between sedentary and wheel-access animals ($\alpha = 0.05$). Here, in a sample of females, no such effects were found (Table 1). In a sample of older female mice (20 months of wheel access; Middleton et al. 2008b), activity similarly produced no detectable effect on skeletal geometry. At the time, we hypothesized that this pattern resulted from the advanced age and presumed post-reproductive status of the mice. However, the pattern observed here suggests a broader pattern of attenuation in osteogenic response to exercise in female mice, despite the fact that female mice, on average, run more than males. A priority for future studies will be simultaneous analyses of both sexes housed under identical conditions.

Nanoindentation

Repeatability of nanoindentation on bone and identification of outliers

Reduced modulus of bone measured by nanoindentation is locally consistent, with repeatability ranging from 0.66 to 0.73. So far as we know, these are the first reported values for repeatability of nanoindentation results for bone. In studies of homogeneous materials, nanoindentation produces highly repeatable measurements, and with increasing heterogeneity, significantly more variability (Jang & Matsubara, 2005). As a consequence, we suggest that a portion of the variability we observe in our sample after the removal of statistical outliers is due to bone anisotropy (Radovic et al. 2004). Because of high repeatability and independence of indents (lack of a significant indentation sequence effect), we used a mean of the nine indents for the majority of statistical tests. We used a preliminary ANCOVA to objectively detect statistical outliers, defining those with standardized residuals greater or less than 3.5 as outliers. With this cutoff, we retained 1672 of 1694 indents (98.7%). A more restrictive subset of indents could be used, but our discovery of significant among-quadrant stiffness suggests that our method is robust. Even after calculating a mean stiffness per quadrant, nanoindentation appears sufficiently sensitive to detect mouse-to-mouse and among-quadrant (within mouse) variation in stiffness (Table 2; see next section).

Applicability of microscale mechanical properties studies

Nanoindentation is a robust and powerful technique for assessing the micromechanical properties of bone (Rho et al. 1997, 1999a). In addition to comparative studies such as the one described here, nanoindentation can be used to assess regional heterogeneity in E_r. As we have shown (Table 3; Fig. 2), material properties may vary within the cortex of a given bone, in addition to the variation in material properties that has been documented among different types of bone (Rho et al. 1997, 1999a,b; Zysset et al. 1999) and among regions in a particular bone, such as the tibia (Fan et al. 2002). Here, we have examined modulus variation in the mid-cortex of the femoral diaphysis, but there remain other spatial dimensions along with mineralization and hence modulus may vary; little is known about material properties around the periosteal or endosteal circumferences of the diaphysis, along the longitudinal axis, or in subchondral bone. These regions are deserving of study to fully understand variation in material properties in the skeleton. Such data would be beneficial for a full understanding of the micro-scale mechanics of bone in a variety of ways, including, for example, finite element modeling studies. With expanded access of μCT, geometrically accurate models can be constructed with increasing ease (Rüegsegger, 2001), and the most accurate finite element models should be able to account for bone anisotropy and regional variation in moduli.

Intra-bone regional stiffness

Using micromechanical testing, Ramasamy & Akkus (2007) found that femoral cortical bone in the anterior quadrant was significantly stiffer when loaded in tension than bone in the posterior quadrant in Swiss Webster mice. In the present study, we used a compressive test, nanoindentation, to compare all four quadrants. As in our sample of mice described herein, Ramasamy & Akkus (2007) found no differences in the compressive properties of the anterior and posterior quadrants.

Direct *in vivo* measurement of bone strain from the long bones of dogs and horses (Rubin & Lanyon, 1982), chickens (Biewener et al. 1986) and rats (Mosley et al. 1997) has shown that convex regions of long bones are loaded in tension and concave areas in compression. Because bone has been shown to respond adaptively to the local loading environment (van der Meulen et al. 1993; van der Meulen & Huiskes, 2002), anterior and posterior quadrants should therefore differ in mechanical properties.

Although at least an order of magnitude smaller in body mass than any dogs or horses, mice possess femora that are nonetheless similar in shape and overall curvature. Compressive loading of the bone as a whole, as would be experienced during locomotion, will cause the anteriorly convex surface to experience tension and the posterior surface to experience primarily compression (Biewener et al. 1983). However, because of logistical difficulties of instrumenting small bones with strain gauges, only two studies have reported *in vivo* bone strains in mice. De Souza et al. (2005) recorded strains from the tibia, and Lee et al. (2002) recorded strains from the ulna. Due to the size of the bones, only a single element strain gauge was used in both studies. As such, the pattern of *in vivo* bone strain, e.g. bending vs. torsional loads, in the mouse femur has yet to be documented empirically.

Differences in mineralization patterns between small and large mammals may result from variation in posture and mechanical loading (Biewener, 1983; Fischer et al. 2002; Witte et al. 2002), from differences in physiology (e.g. metabolic rate, mineral metabolism; Taylor et al. 1970), or from a combination of both. Many authors (e.g. Taylor, 1998, 2000; Taylor et al. 1999; Martin, 2000, 2007; Taylor & Kuiper, 2001; Bigley et al. 2007) have observed that bone remodeling is dependent on a threshold volume of bone that is larger than the entire mouse femur. If bone remodeling occurs in this manner for mammals of all sizes, then the limb bones of small mammals cannot remodel in the same manner as those of large mammals. In small mammals, bone strength may be more dependent on patterns of cortical bone growth that can differentially thicken specific

regions of the cortex, and/or upon collagen fiber orientation (e.g. Skedros & Hunt, 2004; Skedros et al. 2009). Studies of relative bone growth rates and comparisons of collagen fiber orientation between wheel-exercised and control mice are may shed light on the relevance of these phenomena for explaining the patterns observed here.

Bone mineralization in mice bred for high levels of voluntary wheel running

We observed no significant differences in either morphometric traits or bone stiffness attributable to an exercise effect in this population of female mice, although we do find significant differences attributable to the selection regime (Tables 1 and 2). The former result is surprising, considering the extensive literature demonstrating osteogenic responses to mechanical loading (e.g. Carter, 1982; Lanyon et al. 1982; Rubin, 1984; Rubin & Lanyon, 1985; Carter et al. 1987; Frost, 1990, 2003; Lanyon, 1993; Huiskes et al. 2000; Kodama et al. 2000; Parfitt, 2004; Kesavan et al. 2006, 2007). Although wheel running likely engenders smaller loads than artificially produced three- or four-point bending, Kelly et al. (2006) did find significant effects of activity on bone morphology in male mice (e.g. larger femoral heads, wider distal femoral condyles, larger anteroposterior and mediolateral femoral diameters). Although we are not able to rule out the role of increased home-cage activity in HR mice (Malisch et al. 2009) in muting bone's response to wheel-running, two distinctive physiological characteristics in female HR mice suggest that the mechanical adaptation of the skeleton to the mechanical environment may be constrained in specific ways in female HR mice.

First, in at least one sample of female HR mice from this artificial selection experiment, levels of circulating leptin were significantly lower than in C mice (Girard et al. 2007; also see Vaanholt et al. 2007, 2008). This change may lead to decreased bone mineralization, as has been observed in some studies of leptin-deficient or leptin-insensitive mice (Steppan et al. 2000; Cornish et al. 2002; but for conflicting results also see Ducy et al. 2000; Karsenty, 2006). Secondly, female HR mice in the selection experiment appear to have altered signaling in the cannabinoid receptor CB1 pathway (Keeney et al. 2008). Recently, both the CB1 (Tam et al. 2006, 2008; Bab, 2007; Bab & Zimmer, 2008; Idris et al. 2009) and CB2 (Idris et al. 2005; Ofek et al. 2006; Rossi et al. 2009) endocannabinoid receptor pathways have been implicated in the regulation of bone mass. CB1-null mice exhibit an increased bone mass phenotype, but bones in male and female mice respond differently, with males generally showing a greater phenotypic response than females (Tam et al. 2006). Such sex-specific effects of CB1 signaling may account for the variation we have observed in skeletal responses to mechanical loading in distinct, sex-specific populations of mice that are part of this selection experiment.

We hypothesize that the nearly threefold increased number of wheel revolutions observed in HR mice compared to C mice, as well as increased home-cage activity (Garland, 2003; Malisch et al. 2008, 2009), may compensate for the deleterious effects on bone mineralization of decreased leptin levels and altered signaling in the CB1 pathway. However, muscular forces during these routine activities might provide the 'typical peak voluntary mechanical loads' (Frost, 2003) required to maintain bone integrity. Future studies will explore the roles of leptin and the CB1 pathway in establishment and maintenance of bone macro- and microstructure.

Acknowledgements

The authors thank J. Casey and D. C. Moore in the Bioengineering Laboratory at Rhode Island Hospital for assistance with μCT scanning. This work was supported by NSF IOB-0543429 to T. Garland Jr, NSF CMMI-0421199 and NSF CMMI-0824601 to P. R. Guduru, and NIH 1F32AR053008-01 from the National Institute of Arthritis and Musculoskeletal and Skin Diseases to K. M. Middleton.

References

Akhter MP, Fan Z, Rho JY (2004) Bone intrinsic material properties in three inbred mouse strains. *Calcif Tissue Int* **75**, 416–420.

Amanat N, He LH, Swain MV, et al. (2008) The effect of zoledronic acid on the intrinsic material properties of healing bone: an indentation study. *Med Eng Physics* **30**, 843–847.

Bab IA (2007) Regulation of skeletal remodeling by the endocannabinoid system. *Ann N Y Acad Sci* **1116**, 414–422.

Bab IA, Zimmer A (2008) Cannabinoid receptors and the regulation of bone mass. *Br J Pharmacol* **153**, 182–188.

Babij P, Zhao W, Small C, et al. (2003) High bone mass in mice expressing a mutant LRP5 gene. *J Bone Miner Res* **18**, 960–974.

Beamer WG, Shultz KL, Ackert-Bicknell CL, et al. (2007) Genetic dissection of mouse distal chromosome 1 reveals three linked BMD QTLs with sex-dependent regulation of bone phenotypes. *J Bone Miner Res* **22**, 1187–1196.

Bennett AF (2003) Experimental evolution and the Krogh Principle: generating biological novelty for functional and genetic analyses. *Physiol Biochem Zool* **76**, 1–11.

Biewener AA (1983) Locomotory stresses in the limb bones of two small mammals: the ground squirrel and chipmunk. *J Exp Biol* **103**, 131–154.

Biewener AA, Thomason J, Lanyon LE (1983) Mechanics of locomotion and jumping in the forelimb of the horse (*Equus*): *in vivo* stress developed in the radius and metacarpus. *J Zool Lond* **201**, 67–82.

Biewener AA, Swartz SM, Bertram JEA (1986) Bone modeling during growth: dynamic strain equilibrium in the chick tibiotarsus. *Calcif Tissue Int* **39**, 390–395.

Bigley RF, Gibeling JC, Stover SM, et al. (2007) Volume effects on fatigue life of equine cortical bone. *J Biomech* **40**, 3548–3554.

Bower AL, Lang DH, Vogler GP, et al. (2006) QTL analysis of trabecular bone in BXD F_2 and RI mice. *J Bone Miner Res* **21**, 1267–1275.

Broz JJ, Simske SJ, Greenberg AR, et al. (1993) Effects of rehydration state on the flexural properties of whole mouse long bones. *J Biomech Eng* **115**, 447–449.

Carlson KJ, Judex S (2007) Increased non-linear locomotion alters diaphyseal bone shape. *J Exp Biol* **210**, 3117–3125.

Carter DR (1982) The relationship between in vivo strains and cortical bone remodeling. *Crit Rev Biomed Eng* **8**, 1–28.

Carter DR, Fyhrie DP, Whalen RT (1987) Trabecular bone density and loading history: regulation of connective tissue biology by mechanical energy. *J Biomech* **20**, 785–794.

Carter PA, Swallow JG, Davis SJ, et al. (2000) Nesting behavior of house mice (*Mus domesticus*) selected for increased wheel-running activity. *Behav Genet* **30**, 85–94.

Cornish J, Callon KE, Bava U, et al. (2002) Leptin directly regulates bone cell function in vitro and reduces bone fragility in vivo. *J Endocrinol* **175**, 405–415.

Curran-Everett D (2000) Multiple comparison: philosophies and illustrations. *Am J Physiol Reg Integr Comp Physiol* **279**, r1–r8.

Curran-Everett D, Benos DJ (2004) Guidelines for reporting statistics in journals published by the American Physiological Society. *J Appl Physiol* **97**, 457–459.

Currey JD (2003) The many adaptations of bone. *J Biomech* **36**, 1487–1495.

De Souza RL, Matsuura M, Eckstein F, et al. (2005) Non-invasive axial loading of mouse tibiae increases cortical bone formation and modifies trabecular organization: a new model to study cortical and cancellous compartments in a single loaded element. *Bone* **37**, 810–818.

Ducy P, Amling M, Takeda S, et al. (2000) Leptin inhibits bone formation through a hypothalamic relay: a central control on bone mass. *Cell* **100**, 197–207.

Dumke CL, Rhodes JS, Garland T Jr, et al. (2001) Genetic selection of mice for high voluntary wheel running: effect on skeletal muscle glucose uptake. *J Appl Physiol* **91**, 1289–1297.

Eisen EJ (1987) Selection for components related to body composition in mice: direct responses. *Theor Appl Genet* **74**, 793–801.

Eisen EJ (1992) Restricted index selection in mice designed to change body fat without changing body weight: direct responses. *Theor Appl Genet* **83**, 973–980.

Eisen EJ, Benyon LS, Douglas JA (1995) Long-term restricted index selection in mice designed to change fat content without changing body size. *Theor Appl Genet* **91**, 340–345.

Evans FG, Lebow M (1951) Regional difference in some of the physical properties of the human femur. *J Appl Physiol* **3**, 563–572.

Fan Z, Swadener JG, Rho JY, et al. (2002) Anisotropic properties of human tibial cortical bone as measured by nanoindentation. *J Orthop Res* **20**, 806–810.

Fan Z, Smith PA, Harris GF, et al. (2007) Comparison of nanoindentation measurements between osteogenesis imperfecta Type III and Type IV and between different anatomic locations (femur/tibia versus iliac crest). *Conn Tiss Res* **48**, 70–75.

Fischer MS, Schilling N, Schmidt M, et al. (2002) Basic limb kinematics of small therian mammals. *J Exp Biol* **205**, 1315–1338.

Frost HM (1990) Skeletal structural adaptations to mechanical usage (SATMU): 4. Mechanical influences on intact fibrous tissues. *Anat Rec* **226**, 433–439.

Frost HM (2003) Bone's mechanostat: a 2003 update. *Anat Rec A* **275**, 1081–1101.

Gammie SC, Hasen NS, Rhodes JS, et al. (2003) Predatory aggression, but not maternal or intermale aggression, is associated with high voluntary wheel-running behavior. *Horm Behav* **44**, 209–221.

Garland T Jr (2003) Selection experiments: an under-utilized tool in biomechanics and organismal biology. In *Vertebrate Biomechanics and Evolution* (eds Bels VL, Gasc J-P, Casinos A), pp. 23–56. Oxford: BIOS Scientific Publishers, Ltd.

Garland T Jr, Freeman PW (2005) Selective breeding for high endurance running increases hindlimb symmetry. *Evolution* **59**, 1851–1854.

Garland T Jr, Kelly SA (2006) Phenotypic plasticity and experimental evolution. *J Exp Biol* **209**, 2344–2361.

Garland T Jr, Morgan MT, Swallow JG, et al. (2002) Evolution of a small-muscle polymorphism in line of house mice selected for high activity levels. *Evolution* **56**, 1267–1275.

Girard I, Garland T Jr (2002) Plasma corticosterone response to acute and chronic voluntary exercise in female house mice. *J Appl Physiol* **92**, 1553–1561.

Girard IA, Rezende EL, Garland T Jr (2007) Leptin levels and body composition of mice selectively bred for high voluntary locomotor activity. *Physiol Biochem Zool* **80**, 568–579.

Guderley H, Houle-Leroy P, Diffee GM, et al. (2006) Morphometry, ultrastructure, myosin isoforms, and metabolic capacities of the 'mini muscles' favoured by selection for high activity in house mice. *Comp Biochem Physiol B* **144**, 271–282.

Guderley H, Joanisse DR, Mokas S, et al. (2008) Altered fibre types in gastrocnemius muscle of high wheel-running selected mice with mini-muscle phenotypes. *Comp Biochem Physiol B* **149**, 490–500.

Hamrick MW, McPherron AC, Lovejoy CO, et al. (2000) Femoral morphology and cross-sectional geometry of adult myostatin-deficient mice. *Bone* **27**, 343–349.

Hamrick MW, Samaddar T, Pennington C, et al. (2006) Increased muscle mass with myostatin deficiency improves gains in bone strength with exercise. *J Bone Miner Res* **21**, 477–483.

Hannon RM, Kelly SA, Middleton KM, et al. (2008) Phenotypic effects of the 'mini-muscle' allele in a large HR x C57BL/6J mouse backcross. *J Hered* **99**, 349–354.

Hartmann J, Garland T Jr, Hannon RM, et al. (2008) Fine mapping of 'mini-muscle', a recessive mutation causing reduced hind-limb muscle mass in mice. *J Hered* **99**, 679–687.

Hengsberger S, Kulik A, Zysset PK (2002) Nanoindentation discriminates the elastic properties of individual human bone lamellae under dry and physiological conditions. *Bone* **30**, 178–184.

Houle-Leroy P, Guderley H, Swallow JG, et al. (2003) Artificial selection for high activity favors mighty mini-muscle in house mice. *Am J Physiol Reg Integr Comp Physiol* **284**, R433–R443.

Huiskes R, Ruimerman R, van Lenthe GH, et al. (2000) Effects of mechanical forces on maintenance and adaptation of form in trabecular bone. *Nature* **405**, 704–706.

Idris AI, van't Hof RJ, Greig IR, et al. (2005) Regulation of bone mass, bone loss and osteoclast activity by cannabinoid receptors. *Nat Med* **11**, 774–779.

Idris AI, Sophocleous A, Landao-Bassonga E, et al. (2009) Cannabinoid receptor type 1 protects against age-related osteoporosis by regulating osteoblast and adipocyte differentiation in marrow stromal cells. *Cell Metab* **10**, 139–147.

Jang BK, Matsubara H (2005) Influence of porosity on hardness and Young's modulus of nanoporous EB-PVD TBCs by nanoindentation. *Mater Lett* **59**, 3462–3466.

Ji B, Gao H (2004) Mechanical properties of nanostructure of biological materials. *J Mech Phys Solids* **52**, 1963–1990.

Jiao Y, Chiu H, Fan Z, et al. (2007) Quantitative trait loci that determine mouse tibial nanoindentation properties in an F_2 population derived from C57BL/6J X C3H/Hej. *Calcif Tissue Int* **80**, 383–390.

Karsenty G (2006) Convergence between bone and energy homeostases: leptin regulation of bone mass. *Cell Metab* **4**, 341–348.

Kavukcuoglu NB, Denhardt DT, Guzelsu N, et al. (2007) Osteopontin deficiency and aging on nanomechanics of mouse bone. *J Biomed Mater Res A* **83**, 136–144.

Keeney BK, Raichlen DA, Meek TH, et al. (2008) Differential response to a selective cannabinoid receptor antagonist (SR141716: Rimonabant) in female mice from lines selectively bred for high voluntary wheel-running behaviour. *Behav Pharmacol* **19**, 812–820.

Kelly SA, Czech PP, Wight JT, et al. (2006) Experimental evolution and phenotypic plasticity of hindlimb bones in high-activity house mice. *J Morph* **267**, 360–374.

Kesavan C, Mohan S, Oberholtzer S, et al. (2005) Mechanical loading-induced gene expression and BMD changes are different in two inbred mouse strains. *J Appl Physiol* **99**, 1951–1957.

Kesavan C, Mohan S, Srivastava AK, et al. (2006) Identification of genetic loci that regulate bone adaptive response to mechanical loading in C57BL/6J and C3H/Hej mice intercross. *Bone* **39**, 634–643.

Kesavan C, Baylink DJ, Kapoor S, et al. (2007) Novel loci regulating bone anabolic response to loading: expression QTL analysis in C57BL/6J x C3H/Hej mice cross. *Bone* **41**, 223–230.

Kodama Y, Umemura Y, Nagasawa S, et al. (2000) Exercise and mechanical loading increase periosteal bone formation and whole bone strength in C57BL/6J but not in C3H/Hej mice. *Calcif Tissue Int* **66**, 298–306.

Koller DL, Schreifer J, Sun Q, et al. (2003) Genetic effects for femoral biomechanics, structure, and density in C57BL/6J and C3H/Hej inbred mouse strains. *J Bone Miner Res* **18**, 1758–1765.

Lakes R (1993) Materials with structural hierarchy. *Nature* **361**, 511–515.

Lang DH, Sharkey NA, Mack HA, et al. (2005) Quantitative trait loci analysis of structural and material skeletal phenotypes in C57BL/6J and DBA/2 second-generation and recombinant inbred mice. *J Bone Miner Res* **20**, 88–99.

Lanyon LE (1993) Osteocytes, strain detection, bone modeling and remodeling. *Calcif Tissue Int* **53**, S102–S106.

Lanyon LE, Goodship AE, Pye CJ, et al. (1982) Mechanically adaptive bone remodelling. *J Biomech* **15**, 141–154.

Lee KCL, Maxwell A, Lanyon LE (2002) Validation of a technique for studying functional adaptation of the mouse ulna in response to mechanical loading. *Bone* **31**, 1–9.

Leong PL, Morgan EF (2008) Measurement of fracture callus material properties via nanoindentation. *Acta Biomat* **4**, 1569–1575.

Lessels CM, Boag PT (1987) Unrepeatable repeatabilities: a common mistake. *Auk* **104**, 116–121.

MacDonald BT, Joiner DM, Oyserman SM, et al. (2007) Bone mass is inversely proportional to *Dkk1* levels in mice. *Bone* **41**, 331–339.

Malisch JL, Saltzman W, Gomes FR, et al. (2007) Baseline and stress-induced plasma corticosterone concentrations of mice selectively bred for high voluntary wheel running. *Physiol Biochem Zool* **80**, 146–156.

Malisch JL, Breuner C, Gomes FR, et al. (2008) Circadian pattern of total and free corticosterone concentrations, corticosteroid-binding globulin, and physical activity in mice selectively bred for high voluntary wheel-running behavior. *Gen Comp Endocrinol* **156**, 210–217.

Malisch JL, Breuner CW, Kolb EM, et al. (2009) Behavioral despair and home-cage activity in mice with chronically elevated baseline corticosterone concentrations. *Behav Genet* **39**, 192–209.

Martin RB (2000) Toward a unifying theory of bone remodeling. *Bone* **26**, 1–6.

Martin RB (2007) The importance of mechanical loading in bone biology and medicine. *J Musculoskelet Neuronal Interact* **7**, 48–53.

van der Meulen MCH, Huiskes R (2002) Why mechanobiology? A survey article. *J Biomech* **35**, 401–414.

van der Meulen MCH, Beaupré GS, Carter DR (1993) Mechanobiologic influences in long bone cross-sectional growth. *Bone* **14**, 635–642.

Middleton KM, Kelly SA, Garland T Jr (2008a) Selective breeding as a tool to probe skeletal response to high voluntary locomotor activity in mice. *Integr Comp Bio* **48**, 394–410.

Middleton KM, Shubin CE, Moore DC, et al. (2008b) The relative importance of genetics and phenotypic plasticity in dictating bone morphology and mechanics in aged mice: evidence from an artificial selection experiment. *Zoology* **111**, 135–147.

Mosley JR, March BM, Lynch J, et al. (1997) Strain magnitude related changes in whole bone architecture in growing rats. *Bone* **20**, 191–198.

Nazarian A, von Stechow D, Zurakowski D, et al. (2008) Bone volume fraction explains the variation in strength and stiffness of cancellous bone affected by metastatic cancer and osteoporosis. *Calcif Tissue Int* **83**, 368–379.

Ofek O, Karsak M, Leclerc N, et al. (2006) Peripheral cannabinoid receptor, CB2, regulates bone mass. *Proc Natl Acad Sci U S A* **103**, 696–701.

Oliver WC, Pharr GM (1992) An improved technique for determining hardness and elastic modulus using load and displacement-sensing indentation systems. *J Mater Res* **7**, 1564–1583.

Parfitt AM (2004) What is the normal rate for bone remodeling? *Bone* **35**, 1–3.

R Core Development Team (2008) *R: A Language and Environment for Statistical Computing*. R Foundation for Statistical Computing; Vienna. Available at: http://www.R-project.org.

Radovic M, Lara-Curzio E, Riester L (2004) Comparison of different experimental techniques for determination of elastic properties of solids. *Mater Sci Eng A* **368**, 56–70.

Ralston SH, Galwey N, MacKay I, et al. (2005) Loci for regulation of bone mineral density in men and women identified by genome wide linkage scan: the FAMOS study. *Hum Mol Genet* **14**, 943–951.

Ramasamy JG, Akkus O (2007) Local variations in the micromechanical properties of mouse femur: the involvement of collagen fiber orientation and mineralization. *J Biomech* **40**, 910–918.

Rezende EL, Garland T Jr, Chappell MA, et al. (2006a) Maximum aerobic performance in lines of *Mus* selected for high wheel-

running activity: effects of selection, oxygen availability and the mini-muscle phenotype. *J Exp Biol* **209**, 115–127.

Rezende EL, Kelly SA, Gomes FR, et al. (2006b) Effects of size, sex, and voluntary running speeds on costs of locomotion in lines of laboratory mice selectively bred for high wheel-running activity. *Physiol Biochem Zool* **79**, 83–99.

Rho JY, Pharr GM (1999) Effects of drying on the mechanical properties of bovine femur measured by nanoindentation. *J Mater Sci Mater Med* **10**, 485–488.

Rho JY, Tsui TY, Pharr GM (1997) Elastic properties of human cortical and trabecular lamellar bone measured by nanoindentation. *Biomaterials* **18**, 1325–1330.

Rho JY, Roy ME, Tsui TY, et al. (1999a) Elastic properties of microstructural components of human bone tissue as measured by nanoindentation. *J Biomed Mat Res* **45**, 48–54.

Rho JY, Zioupos P, Currey JD, et al. (1999b) Variations in the individual thick lamellar properties within osteons by nanoindentation. *Bone* **25**, 295–300.

Rho JY, Zioupos P, Currey JD, et al. (2002) Microstructural elasticity and regional heterogeneity in human femoral bone of various ages examined by nano-indentation. *J Biomech* **35**, 189–198.

Rhodes JS, Gammie SC, Garland T Jr (2005) Neurobiology of mice selected for high voluntary wheel-running activity. *Integr Comp Bio* **45**, 438–455.

Robling AG, Turner CH (2002) Mechanotransduction in bone: genetic effects on mechanosensitivity in mice. *Bone* **31**, 562–569.

Robling AG, Li J, Shultz KL, et al. (2003) Evidence for a skeletal mechanosensitivity gene on mouse chromosome 4. *FASEB J* **17**, 324–326.

Robling AG, Warden SJ, Shultz KL, et al. (2007) Genetic effects on bone mechanotransduction in congenic mice harboring bone size and strength quantitative trait loci. *J Bone Miner Res* **22**, 984–991.

Rossi F, Siniscalco D, Luongo L, et al. (2009) The endovanilloid/endocannabinoid system in human osteoclasts: possible involvement in bone formation and resorption. *Bone* **44**, 476–484.

Roy ME, Rho JY, Tsui TY, et al. (1999) Mechanical and morphological variation of the human lumbar vertebral cortical and trabecular bone. *J Biomed Mat Res* **44**, 191–197.

Rubin CT (1984) Skeletal strain and the functional significance of bone architecture. *Calcif Tissue Int* **36**, S11–S18.

Rubin CT, Lanyon LE (1982) Limb mechanics as a function of speed and gait: a study of functional strains in the radius and tibia of horse and dog. *J Exp Biol* **101**, 187–211.

Rubin CT, Lanyon LE (1985) Regulation of bone mass by mechanical strain magnitude. *Calcif Tissue Int* **37**, 411–417.

Rüegsegger P (2001) Imaging of bone structure. In *Bone Mechanics Handbook* (ed. Cowin SC), pp. 9-1–9-24. Boca Raton, FL: CRC Press.

Ryan SD, Williams JL (1989) Tensile testing of rodlike trabeculae excised from bovine femoral bone. *J Biomech* **22**, 351–355.

Silva MJ, Brodt MD, Fan Z, et al. (2004) Nanoindentation and whole-bone bending estimates of material properties in bones from the senescence accelerated mouse SAMP6. *J Biomech* **37**, 1639–1646.

Skedros JG, Hunt KJ (2004) Does the degree of laminarity correlate with site-specific differences in collagen fibre orientation in primary bone? An evaluation in the turkey ulna diaphysis. *J Anat* **205**, 121–134.

Skedros JG, Mendenhall SD, Kiser CJ, et al. (2009) Interpreting cortical bone adaptation and load history by quantifying osteon morphotypes in circularly polarized light images. *Bone* **44**, 392–403.

Steppan CM, Crawford DT, Chidsey-Frink KL, et al. (2000) Leptin is a potent stimulator of bone growth in *ob/ob* mice. *Regul Pept* **92**, 73–78.

Storey JD (2002) A direct approach to false discovery rates. *J R Stat Soc Series B Stat Methodol* **64**, 479–498.

Swallow JG, Carter PA, Garland T Jr (1998) Artificial selection for increased wheel-running behavior in house mice. *Behav Genet* **28**, 227–237.

Swallow JG, Koteja P, Carter PA, et al. (1999) Artificial selection for increased wheel-running activity in house mice results in decreased body mass at maturity. *J Exp Biol* **202**, 2513–2520.

Swallow JG, Hayes JP, Koteja P, et al. (2009) Selection experiments and experimental evolution of performance and physiology. In *Experimental Evolution: Concepts, Methods, and Applications of Selection Experiments* (eds Garland T Jr, Rose MR), pp. 301–351. Berkeley: University of California Press.

Syme DA, Evashuk K, Grintuch B, et al. (2005) Contractile abilities of normal and 'mini' triceps surae muscle from mice (*Mus domesticus*) selectively bred for high voluntary wheel running. *J Appl Physiol* **99**, 1308–1316.

Tai K, Dao M, Suresh S, et al. (2007) Nanoscale heterogeneity promotes energy dissipation in bone. *Nat Mater* **6**, 454–462.

Tam J, Ofek O, Fride E, et al. (2006) Involvement of neuronal cannabinoid receptor CB1 in regulation of bone mass and bone remodeling. *Mol Pharmacol* **70**, 786–792.

Tam J, Trembovler V, Di Marzo V, et al. (2008) The cannabinoid CB1 receptor regulates bone formation by modulating adrenergic signaling. *FASEB J* **22**, 285–294.

Taylor C, Schmidt-Nielsen K, Raab J (1970) Scaling of the energetic cost of running to body size in mammals. *Am J Physiol* **219**, 1104–1107.

Taylor D (1998) Fatigue of bone and bones: an analysis based on stressed volume. *J Orthop Res* **16**, 163–169.

Taylor D (2000) Scaling effects in the fatigue strength of bones from different animals. *J Theor Biol* **206**, 299–306.

Taylor D, Kuiper JH (2001) The prediction of stress fractures using a 'stressed volume' concept. *J Orthop Res* **19**, 919–926.

Taylor D, O'Brien FJ, Prina-Mello A, et al. (1999) Compression data on bovine bone confirms that a 'stressed volume' principle explains the variability of fatigue strength results. *J Biomech* **32**, 1199–1203.

Turner CH, Rho JY, Takano Y, et al. (1999) The elastic properties of trabecular and cortical bone tissues are similar: results from two microscopic measurement techniques. *J Biomech* **32**, 437–441.

Vaanholt LM, Meerlo P, Garland T Jr, et al. (2007) Plasma adiponectin is increased in mice selectively bred for high wheel-running activity, but not by wheel running per se. *Horm Metab Res* **39**, 377–383.

Vaanholt LM, Jonas I, Doornbos M, et al. (2008) Metabolic and behavioral responses to high-fat feeding in mice selectively bred for high wheel-running activity. *Int J Obes* **32**, 1566–1575.

Witte H, Biltzinger J, Hackert R, et al. (2002) Torque patterns of the limbs of small therian mammals during locomotion on flat ground. *J Exp Biol* **205**, 1339–1353.

Zysset PK, Guo XE, Hoffler CE, et al. (1999) Elastic modulus and hardness of cortical and trabecular bone lamellae measured by nanoindentation in the human femur. *J Biomech* **32**, 1005–1012.